Lowering down the temperature synthesis of transition metal carbides: the case of niobium carbide

*C.A. Chagas Jr., V. Teixeira da Silva**

NUCAT / PEQ / COPPE
Federal University of Rio de Janeiro
Rio de Janeiro - Brazil

Abstract

Bulk niobium carbide with a surface area as high as 70 m^2g^{-1} has been synthesized by thermal decomposition of niobium guanidate at temperatures ranging from 673 up to 1073 K and used as catalyst for the hydrodesulfurization (HDS) of model compounds at 3 MPa and 643 K. The samples were characterized by X Ray Diffraction, Scanning Electron Microscopy, XANES Nb L_2-edge, and N_2 physisorption. It was seen from XRD that while for decomposition temperatures below 823 K the obtained compounds are amorphous, for temperatures above 873 K the NbC diffraction pattern is clear. The activity results have shown that contrarily to NbC synthesized by TPR and CH_4/H_2, the one obtained by decomposition of niobium guanidate at 923 K is active in HDS reactions.

Introduction

Transition metal carbides have widespread applications because of their unique physical properties such as high melting points, hardness, electrical conductivity, and superconductivity (1). In catalysis, the materials have attracted attention because they display activities similar to those of the noble metals of Group 8–10 for a variety of reactions such as ammonia synthesis (2), hydrogenation (3), methanation, isomerization, and hydrotreating (4).

Traditionally, transition metal carbides are synthesized using a temperature-programmed reaction (TPR) of a metal oxide (e.g., Nb_2O_5, MoO_3, WO_3, etc.) and a gas mixture (in general 20% (v/v) CH_4/H_2). Depending on the desired carbide, different final synthesis temperatures have to be employed. However, at temperatures higher than 923 K methane decomposition takes place ($CH_4 \rightarrow C + 2\ H_2$) and leads to surface contamination by pyrolitic carbon. Depending on the final synthesis temperature, a large amount of pyrolitic carbon is formed and completely covers the surface and thus suppress the catalytic properties. This is the case of NbC which cannot be synthesized using CH4/H2 gas mixtures at temperatures lower than 1173 K and because of the large amounts of pyrolitic carbon presents no activity for hydrotreating reactions.

The main objective of this work was to synthesize NbC by a new methodology, the guanide route, which uses temperatures lower than 1173 K.

Experimental

Synthesis of NbC was done in a two steps procedure. In the first, guanidinium carbonate (Acros) was physically mixed in a mortar with ammoniacal niobium oxalate ($NH_4[NbO(C_2O_4)_2(H_2O)_2]$, CBMM) with a 3:1 niobium:guanidinum ratio. After homogenization, the physical mixture was heated at 423 K for 12 hours, forming the niobium guanidate compound. In the second step, the niobium guanidate (≈ 0,5g) was decomposed under flux of pure He (150 mL min^{-1}) using a temperature program which consisted in raising it at 10 K min^{-1} from 298 K to a desired final temperature and keeping it for a 2 hour period. After that, the temperature was dropped to room temperature and the obtained material was catalytically evaluated at 3 MPa and 643 K for the hydrodesulphurization of thiophene, benzothiopene or dibenzothiopne. The samples used in characterization (XRD, SEM, XANES Nb L_2-edge and N_2 physisorption) were passivated at room temperature with a 0.5% O_2 / He (50 mL min^{-1}) mixture prior to atmosphere exposure.

Results and Discussion

The XRD patterns obtained for the samples synthesized at different temperatures reveal that while the materials obtained at 673 and 723 K are amorphous, the sample synthesized at 823 K presents a small diffraction peak at $2\theta \approx 34^o$ which increases in intensity as the decomposition temperature augments. For the sample obtained at 923 K the diffraction peaks of NbC are present. This result reveals that the guanidine route allows the synthesis of NbC at temperatures as low as 923 K and thus presenting a potential advantage over the traditional TPR method4.

The variation of the specific surface area (S_g) increases from 22 $m^2\ g^{-1}$ for the sample synthesized at 673 K to 70 m^2g^{-1} for the one obtained at 923 K. Further increases in the decomposition temperature lead to a decrease in the value of S_g.

The sample synthesized at 923 K was tested as catalyst for the HDS of feeds of tetradecane containing 2 000 ppm of different sulfur model compounds. The activity results have shown that the NbC presented an initial deactivation with the HDS conversions for thiophene, benzothiophene and dibenzothiophene being 70, 55 and 40%, respectively, after a 24 hour reaction period.

Conclusions

Niobium carbide free of superficial carbon can be synthesized at temperatures as low as 923 K by a new methodology, the guanidine route. The sample obtained at 923 K has a surface area of 70 $m^2g^{-1}$and is active for the HDS of sulfur model compounds.

References

(1) L. E. Toth, ‘‘Transition Metal Carbides and Nitrides.’’ Academic Press, New York, 1971.
(2) M. Boudart, S. T. Oyama, and L. Leclercq, in ‘‘Proceedings, 7th International Congress on Catalysis, Tokyo 1980’’ (T. Seiyama and K. Tanabe, Eds.), Elsevier, Amsterdam, 1981, Vol. 1, p. 578.
(3) I. Kojima, E. Miyazaki, Y. Inoue, and I. Yasumori, J. Catal. 73, (1982) 128.
(4) J. C. Schlatter, S. T. Oyama, J. E. Metcalfe III, and J. M. Lambert Jr., Ind. Eng. Chem. Res. 27, (1988) 1648.

HDS Studies on Phosphide Catalysts

S.T. Oyama[1,2], H.Y. Zhao[1], H.J.-Freund[3], K. Asakura[4], Radoslaw Wlodarczyk[5], Marek Sierka[5]*

[1]Department of Chemical Engineering, Virginia Tech, Blacksburg, Virginia 24061
[2]The University of Tokyo, Department of Chemical Systems Engineering, Tokyo, Japan
[3]Fritz-Haber-Institute of Max-Plank-Society, D-14195, Berlin, Germany
[4]Catalysis Research Center and Department of Quantum Science and Technology, Hokkaido University, Kita 21-10 Sapporo, 001-0021, Japan
[5]Institut für Chemie, Humboldt-Universität zu Berlin, Unter den Linden 6, 10099 Berlin, Germany

Introduction

The removal of sulfur from petroleum feedstocks is an area of great importance, and novel catalysts for hydrodesulfurization (HDS) have been recently reviewed [1]. Among the most active new compositions are transition metal phosphides with activity higher than conventional sulfides based on sites titrated by chemisorptions [2-9]. The activity of common phosphides follows the order:

$$Ni_2P > WP > MoP > CoP > Fe_2P$$

in the simultaneous HDS of dibenzothiophene (3000 ppm S) and HDN of quinoline (2000 ppm N) at 643 K and 3.1 MPa, [10,11]. Unexpectedly, bimetallic phosphides have not shown dramatic activity even though a marked synergy is observed with sulfides. Thus, compounds such as Ni_xMo_yP [12-17] and Ni_xCo_yP [16,18,19] do not display extraordinary activity over their component phosphides. This has been rationalized from the structure of the compounds [9]. The crystal structure of Ni_2P is hexagonal, and contains two types of Ni sites, Ni(1) of tetrahedral coordination and Ni(2) of square pyramidal coordination. A study using extended x-ray absorption fine structure (EXAFS) was conducted in which the number of Ni(2) sites was varied by changing particle size. This showed that these sites were responsible for hydrogenation and had particularly high activity for HDS [9]. The lack of activity of the bimetallic compounds could be understood as due to substitution of the less active element (Mo or Co) in the Ni(2) site.

This investigation employed silica-supported Ni_xFe_yP compounds of different Ni:Fe molar ratios: Ni_2P/SiO_2, NiFeP(3:1)/SiO_2, NiFeP(1:1)/SiO_2, NiFeP(1:3)/SiO_2, and Fe_2P/SiO_2. The NiFe system was examined because Ni_2P and Fe_2P have the same crystal structure, yet Fe_2P is practically inactive in HDS. For this reason, Fe was expected to be useful as a probe for the active sites in Ni_2P. The location of the Fe was determined using EXAFS and theoretical calculations. It was found that both Fe and Ni occupied M(2) sites and high activity was retained. Moreover, the selectivity toward direct desulfurization, the preferred pathway because it consumes minimal hydrogen, increased dramatically.

Experimental

The NiFeP catalysts were prepared by temperature-programmed reduction (TPR), following procedures reported previously [20,21]. Briefly, the synthesis of the catalysts involved two stages. First, solutions of the corresponding metal phosphate precursors were prepared by dissolving appropriate amounts of $Fe(NO_3)_3{\cdot}9H_2O$, $Ni(NO_3)_2{\cdot}6H_2O$, with ammonium phosphate in distilled water, and these solutions were used to impregnate silica EH-5 by the incipient wetness method. Second, the solid phosphates were reduced to phosphides at 2 °C min^{-1} in flowing H_2 [1000 cm^3 (NTP) min^{-1} g^{-1}].

X-ray diffraction (XRD) patterns of the samples were obtained with a Scintag XDS-2000 powder diffractometer operated at 45 kV and 40 mA, using Cu Kα monochromatized radiation (λ= 0.154178 nm). X-ray absorption spectra at the Ni K-edge (8.333 keV) and Fe K-edge (7.112 keV) of reference and catalyst samples were recorded in the energy range 8.233–9.283 keV at beam line X18B at the National Synchrotron Light Source at Brookhaven National Laboratory. The X-ray ring at the National Synchrotron Light Source has a flux of 1×10^{10} photons s^{-1} at 100 mA and 2.5 GeV. The monochromator is equipped with a Si(111) channel-cut single crystal and has an energy range capability of 5.8–40 keV. Samples before reaction (labeled fresh) were reduced in hydrogen as for the reactivity studies, and were loaded into cells with Kapton windows without exposure to the atmosphere.

Hydrotreating activities of the samples were measured in a three-phase, packed-bed reactor operated at 3.1 MPa and 613K with a model feed liquid containing 500 ppm sulfur as 4,6-DMDBT, 3000 ppm sulfur as dimethyl disulfide, 200 ppm nitrogen as quinoline, 1 wt.% tetralin, 0.5 wt.% n-octane as internal standard, and balance n-tridecane. The schematic of the testing system was described in an earlier paper [22].

Periodic density functional theory (DFT) calculations were carried out using the Vienna Ab Initio Simulation package (VASP) and the Perdew, Burke and Ernzerhof (PBE) exchange-correlation functional. The calculations were performed using the projector augmented wave method (PAW), originally developed by Blöchl and adapted by Kresse and Joubert. Only the valence electrons were explicitly considered. Optimizations of cell parameters used a 7×7×13 Monkhorst-Pack k-point mesh for the Brillouin-zone sampling and an energy cutoff of 1000 eV for a plane wave basis set. The Pulay stress arising from the incomplete basis set was minimized by restarting the optimization until self-consistency of the total energy was reached. Optimizations of atomic positions for the structures shown in Table 1 were performed with a 4×4×7 Monkhorst-Pack k-point mesh and a plane wave cutoff of 400 eV. Optimizations of atomic positions for the structures shown in Table 2 were performed with a plane wave cutoff of 500 eV. Optimizations of atomic positions for 1x1x2 supercells were performed with 4×4×4 Monkhorst-Pack k-point mesh.

Results and Discussion

The d-spacings for the series of compositions an unsual trend, first decreasing and then increasing with Fe content. This has been reported recently by Bussell and collaborators [23].

Table 1. XRD Analysis of NiFeP/SiO_2 Samples

d-spacing (hkl)/nm	(111)	(201)	(210)
Ni_2P/SiO_2	0.221	0.202	0.191
NiFeP(3:1)/SiO_2	0.219	0.202	0.192
NiFeP(1:1)/SiO_2	0.220	0.202	0.190
NiFeP(1:3)/SiO_2	0.220	0.203	0.192
Fe_2P/SiO_2	0.223	0.205	0.193

Reactivity studies of simultaneous 4,6-dimethyldibenzo-thiophene (4,6-DMDBT) HDS and quinoline HDN were carried out at two different temperatures 300 and 340 ºC (573, 613 K) at the same pressure (3.1 MPa, 450 psig). The Fe_2P/SiO_2 sample deactivated in the course of reaction, as found earlier [21], and results for this sample cannot be presented. Various liquid feeds with the different compositions were introduced in sequence in the course

of the reaction test. Initially, 0.05% S in form of 4,6-DMDBT, 0.3% S as DMDS, 0.02% N as quinoline dissolved in tridecane were introduced at 573 K (300 ^{o}C). The Ni_2P/SiO_2 catalyst exhibited high reactivity and stability with a 4,6-DMDBT conversion of 97-99%. The NiFeP(3:1)/SiO_2 sample had an HDS conversion of around 90% and showed a slight decline in activity The NiFeP(1:1) /SiO_2 sample had a HDS conversion of only about 40% and also exhibited deactivation. With increase in Fe content, the activity of the catalysts became lower. This is consistent with an earlier study of dibenzothiophene HDS which showed that Fe_2P had a much lower intrinsic activity than Ni_2P [21]. After 80 h on stream time the temperature was increased up to 613 K (340 ^{o}C) under the same feed and this did not affect the HDS activity of Ni_2P/SiO_2, which was already operating at very high conversion. However, the higher temperature increased the HDS activity of NiFeP(3:1)/SiO_2 to a conversion level of 95% and led to a substantial enhancement in HDS activity for NiFeP(1:1)/SiO_2 to a conversion level of 90 %. After 85 h a feed with an additional 0.3 % S as DMDS was introduced (Fig. 5, section iii). The activity of the Ni_2P/SiO_2 did not show much difference, however, the 4,6-DMDBT conversions with NiFeP/SiO_2 (3:1) and NiFeP/SiO_2 (1:1) decreased to 90% and 85% respectively. The small effect of sulfur on the performance of Ni_2P/SiO_2 had been reported earlier [24,25,26].

Fourier transform infrared (FTIR) spectroscopy of adsorbed CO was used as a probe of the surface. The CO stretching frequency shifted to lower wavenumbers with increasing Fe content consistent with electron donation from Fe to Ni, which would weaken the CO bond by back-donation to its antibonding orbitals. The CO peak intensity (I in absorbance units per mg) decreased with Fe content, indicating that the surface was increasingly occupied by Fe, which as a phosphide does not chemisorb CO appreciably.

What was totally unexpected was a change in selectivity (Table 2). According to the published literature [27,28], there are three major products formed from 4,6-DMDBT conversion on the catalysts: (1) 3,3'-dimethylbiphenyl (DMBP), (2) 3-(3'-methylcyclohexyl)toluene (MCHT), and (3) 3,3'-dimethylbicyclohexyl (DMBCH). As a first approximation DMBP can be considered to result from a direct desulfurization (DDS) pathway, whereas the MCHT and DMBCH products from a hydrogenation (HYD) pathway [29,30]. Table 5 shows that the Ni_2P/SiO_2 gave a low DMBP selectivity of 12% and high MCHT and DMBCH selectivity totally accounting for 88%, indicating that Ni_2P/SiO_2 favors the HYD pathway. On the other hand, NiFeP(3:1)/SiO_2 and NiFeP(1:1)/SiO_2 catalysts showed higher DMBP selectivity than that of the hydrogenation products MCHT and DMBCH. The NiFeP(1:1)/SiO_2 sample even gave higher DMBP selectivity of 85% than the 69% selectivity with NiFeP(3:1)/SiO_2. This suggests that Fe intrinsically favors the DDS pathway more than HYD pathway. As the DDS pathway is intrinsically more difficult than the HYD pathway for HDS of 4,6-DMDBT, this rationalizes the decrease in HDS activity in the samples of higher Fe content.

Table 2. Conversion and selectivity for silica-supported nickel phosphide and nickel iron phosphides at 613 K and 3.1 Mpa after 110 h on stream.

Reactants	Type	Conversion/%			Products	Selectivity/%		
		Ni_2P/SiO_2	iFeP(3:1) /SiO_2	NiFeP(1:1) /SiO_2		Ni_2P/SiO_2	iFeP(3:1) /SiO_2	NiFeP(1:1) /SiO_2
4,6-DMDBT	HDS	99	99	96	3,3`-Dimethybiphenyl	12	69	85
					3-(3`-Methylcyclohexyl)toluene	53	21	11
					3,3`-Dimethylbicylohexyl	35	10	4
Quinoline	HDN	100	100	100	Propylcyclohexane	74	45	37
					propylbenzene	26	55	63

Calculation results for various choices of NiFeP structures with fractional occupations of M(1) and M(2) sites predict that most stable structures contain 50% Ni and Fe in these positions and are energetically preferred over other investigated configurations by at least 1.5 kJ/mol per atom. This is in agreement with the EXAFS results.

Conclusions

1) At low reaction temperature (300 ^{o}C) Ni_2P has excellent activity for the simultaneous HDS of 4,6-dimethyldibenzothiophene (conversion 99%) and the hydrodenitrogenation of quinoline (conversion 100%), while Fe substitution decreases the activity.
2) Analysis by extended x-ray absorption fine structure (EXAFS) analysis and theoretical calculations indicates that both Fe and Ni occupy square pyramidal Ni sites (denoted as Ni(2) sites).
3) The high activity of NiFeP is probably due to a ligand effect with Fe donating electrons to Ni.

Acknowledgement. This work was supported by the US Department of Energy, Office of Basic Energy Sciences, through Grant DE-FG02-963414669.

References

(1) S.T. Oyama, T. Gott, H. Zhao, Y.K. Lee, Catal. Today 143 (2009) 94.
(2) W. R. A. M. Robinson, J. N. M. van Gastel, T. I. Korányi, S. Eijsbouts, J. A. R. van Veen, V. H. J. de Beer, J. Catal. 161 (1996) 539
(3) W. Li, B. Dhandapani, S. T. Oyama, Chem. Lett. (1998) 207.
(4) C. Stinner, R. Prins, Th. Weber, J. Catal. 202 (2001) 187.
(5) V. Zuzaniuk, R. Prins, J. Catal. 219 (2003) 85.
(6) S. T. Oyama, J. Catal. 216 (2003) 343.
(7) S. T. Oyama, Y.-K. Lee, J. Phys. Chem. B *109* (2005) 2109.
(8) Y.-K. Lee and S. T. Oyama, J. Catal. 239 (2006) 376.
(9) S. T. Oyama, Y.-K. Lee, J. Catal. 258 (2008) 393.
(10) X. Wang, Y. Lee, W. J. Chun, S. T. Oyama, F. Requejo, J. Catal., 210 (2002) 207..
(11) P. Clark, X. Wang, S.T.Oyama, J. Catal. 207 (2002) 256.
(12) F. Sun, W. Wu, Z. Wu, J. Guo, Z. Wei, Y. Yang, Z. Jiang, F. Tian, C. Li, J. Catal. 228 (2004) 298.
(13) C. Stinner, R. Prins, Th. Weber, J. Catal. 202 (2001) 187.

(14) J. A. Rodriguez, J.-Y. Kim, J. C. Hanson, S. J. Sawhill, M. E. Bussell, J. Phys. Chem. B (2003) 6276.
(15) D. Ma, T. Xiao, S. Xie, W. Zhou, S. L. Gonzalez-Cortes, M. L. H. Green, Chem. Mater. 16 (2004) 2697.
(16) I.I. Abu, K.J. Smith, J. Catal. 241 (2006) 356.
(17) I.I. Abu, K.J. Smith, Catal. Today 125 (2007) 248.
(18) I.I. Abu, K.J. Smith, Appl. Catal. A: Gen. 328 (2007) 58.
(19) A.W. Burns, A.F. Gaudette, M.E. Bussell, J. Catal. 260 (2008) 262.
(20) J.F. Deng, H. Li, W. Wang, Catal. Today 51 (1999) 113.
(21) X. Wang, P. Clark, S. T. Oyama, J. Catal. 208 (2002) 321.
(22) S. Ramanathan, S.T. Oyama, J. Phys. Chem. 99 (1995) 16365.
(23) A. F. Gaudette, A. W. Burns, J. R. Hayes, M. C. Smith, R. H. Bowker, T. Seda, M. E. Bussell J. Catal. In press.
(24) S.T. Oyama, X. Wang, Y.K. Lee, K. Bando, F.G. Requejo, J. Catal. 210 (2002) 207.
(25) S.T. Oyama, J. Catal. 2106 (2003) 343.
(26) Y. Shu, Y.K. Lee, S.T. Oyama, J. Catal. 236 (2005) 112-121.
(27) V. Vanrysselberghe, G. F. Froment, Ind. Eng. Chem. Res., 35 (1996) 3311..
(28) V. Vanrysselberghe, R. L. Gall, G. F. Froment, Ind. Eng. Chem. Res., 37 (1998) 1235.
(29) J. H. Kim, X. Ma, C. Song, Y.-K. Lee, S. T. Oyama, Energy & Fuels, 19 (2005) 353.
(30) R. Prins, M. Egorava, A. Rothlishberger, Y. Zhao, N. Sivasankar, P. Kukula, Catal. Today 111 (2006) 84.

Design rules for $CoMo/Al_2O_3$ hydrotreating catalysts: how to obtain true type II 'Co-Mo-S'

Emiel J.M. Hensen, A.I. Dugulan, J.A.R. van Veen
Schuit Institute of Catalysis, Eindhoven University of Technology,
P.O. Box 513, NL-5600 MB, Eindhoven, The Netherlands

Introduction

The active phase dispersion and morphology are the most important factors determining the catalytic activity of supported Co(Ni)Mo sulfide hydrotreating catalysts. Topsøe and co-workers have introduced two types of Co-Mo-S phases (1), a Type II phase in which Mo–O–Al linkages with the support are absent with a two times higher activity in gas-phase hydrodesulfurization (HDS) than its incompletely sulfided Type I counterpart (2-4). Complexing agents decrease the Mo-support interactions (5,6) and promote Type II Co-Mo-S phase formation. The extent of type II character of the active phase depends on the Mo loading (6). Despite its importance, it remains difficult to probe spectroscopically the difference between type I and II Co-Mo-S phases. Here we will show that a true type II Co-Mo-S phase for alumina-supported CoMo can only be obtained by using NTA and applying high-pressure sulfidation.

Experimental

Catalyst preparation. Catalysts were prepared by pore-volume impregnation of γ-Al_2O_3 with aqueous solutions of cobalt nitrate and ammonium heptamolybdate. Nitrilotriacetic acid (NTA) was used as complexing agent. For Mössbauer experiments, 50 MBq ^{57}Co was added to the impregnation solution. Except for the NTA-containing samples, the catalysts were calcined prior to sulfidation in H_2S/H_2.

^{57}Co Mössbauer spectroscopy. ^{57}Co MES spectra were recorded using a constant acceleration spectrometer in a triangular mode with a moving single-line $K_4Fe(CN)_6.3H_2O$ absorber enriched in ^{57}Fe. The spectra were analyzed with a Lorentzian fitting procedure. Spectra were recorded for ^{57}Co-enriched CoMo and CoMo-NTA catalysts in an in-situ cell enabling sulfidation at temperatures up to 500˚C and pressures up to 40 bar (7).

XAS experiments. X-ray absorption spectroscopy (XAS) spectra of sulfided CoMo-based catalysts were recorded in a closed cell at the Mo and Co K-edges at the ESRF facility (Dubble, Grenoble). Prior to recording spectra, the catalysts were sulfided at various temperatures and pressures.

Results and Discussion

Sulfidation at elevated pressure improves the sulfidation of the 'Co-Mo-S' phase in alumina-supported catalysts. Calcined catalysts, which have a Type I active 'Co-Mo-S' phase after sulfidation at atmospheric pressure, exhibit a higher HDS activity after high-pressure sulfidation. This is due to partial transformation to a 'Co-Mo-S' phase with an increased Type II character. Full sulfidation remains difficult. Only when Mo-support interactions are minimized in the precursor with NTA it becomes possible to prepare a pure Type II 'Co-Mo-S' phase upon high-pressure sulfidation. Atmospheric pressure sulfidation of a CoMo-NTA catalyst leads to an active 'Co-Mo-S' phase somewhere between the Type I and II. A reasonable indicator of the Type I/II character is the Mo-S coordination number derived from Mo K-edge XAS. From our large dataset, one may abstract the following points regarding the phase I/II behavior of sulfided CoMo catalysts: (i) there is a continuum of active phase 'Co-Mo-S' structures ranging from a less active Type I phase having a strong interaction with the support up to a fully sulfided and possibly well-crystallized Type II 'Co-Mo-S' phase; (ii) a pure Type II end member is obtained after high-pressure sulfidation of a CoMo-NTA catalyst, whereas the earlier Type II phase resulting from sulfidation of CoMo-NTA at atmospheric pressure should now be regarded as a phase with some Type I character.

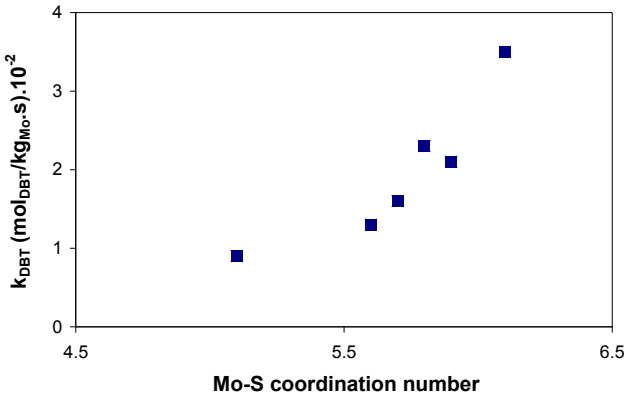

Figure 1. Dibenzothiophene HDS activity as a function of the Mo-S coordination number for a number of $CoMo/Al_2O_3$ catalysts.

Typically, with increasing sulfidation degree of NTA catalysts, stacking of MoS_2 slabs becomes more pronounced. Stacking does not impede gas-phase thiophene HDS as much as it does the gas-phase DBT HDS. This negative effect is reproduced for a set of supported NiMo sulfide catalysts. This could point to some heterogeneity in the distribution of promoter ions on the edges of the slabs in direct contact with the support and the ones on top of that. The HDS activity of CoMo-NTA catalysts sulfided at high pressure with a somewhat stacked MoS_2 morphology may be improved by limiting the stacking of the active phase. The most active catalyst in DBT HDS is a calcined CoMo catalyst and an important explanation seems to be that a large portion of the active phase consists of monolayer slabs. The active phase of this catalyst should be between a Type I and II 'Co-Mo-S' phase and thus further modifications to increase the sulfidation degree whilst keeping the stacking degree low should be the way to improve the activity.

Conclusions

A true type II 'Co-Mo-S' phase in $CoMo/Al_2O_2$ hydrotreating catalysts can be obtained by using chelating agents and high-pressure sulfidation. The small differences in sulfidation degree underlying the extent of type I/II behavior are best probed by the Mo-S coordination number. Besides, the activity in DBT HDS is more influenced by the stacking degree of the MoS_2 phase than is the thiophene HDS. The most active hydrotreating catalysts should be completely sulfided and have a monolayer MoS_2 morphology.

References

(1) Candia, R.; Sorensen, O.; Villadsen, J.; Topsøe, N.-Y.; Clausen, B.S.; Topsøe, H. *Bull. Soc. Chim. Belg.* **1984**, 93, 763.
(2) Topsøe, H.; Clausen, B.S. and Massoth, F.E. in: Anderson, J.R.; Boudart, M. (Eds.), *Hydrotreating Catalysis*, in: Catal. Science Technol., vol. 11, Springer, Berlin, **1996**.
(3) Van Veen, J.A.R.; Gerkema, E.; Van der Kraan, A.M.; Knoester, A. *J. Chem. Soc. Chem. Comm.* **1987**, 1684.
(4) Bouwens, S.M.A.M.; Van Zon, F.B.M.; Van Dijk, M.P.; Van der Kraan, A.M.; De Beer, V.H.J.; Van Veen, J.A.R.; Koningsberger, D.C. *J. Catal.* **1994**, 146, 375.
(5) Van Veen, J.A.R.; Gerkema, E.; Van der Kraan, A.M.; Hendriks; P.A.J.M.; and Beens, H. *J. Catal.* **1992**, 133, 112.
(6) Hensen, E.J.M.; De Beer, V.H.J.; Van Veen, J.A.R.; Van Santen, R.A. *Catal. Lett.* **2002**, 84, 59.
(7) Dugulan, A.I.; Hensen, E.J.M.; and Van Veen, J.A.R. *Catal. Today* **2008**, 130, 126.

SOLID NANOPARTICLES TO STABILIZE WATER/-OIL EMULSIONS AND CATALYZE REACTIONS AT THE LIQUID/LIQUID INTERFACE

*Steven Crossley, Jimmy Faria, Min Shen, Daniel E. Resasco**
University of Oklahoma, School of Chemical Biological and Materials Engineering, Norman OK 73019

Introduction

Pyrolysis oil is a complex mixture of oxygenated compounds with up to ~30-40% of water. Depending on the cooling process used in the condensation of the pyrolysis vapors, the crude bio-oil can generate a biphasic system, in which molecules are distributed, between the two phases, depending on their solubility. It is desirable to conduct reactions at the water/oil interface that can both enhance the fuel value of the molecules and effect phase migration, based on solubility, avoiding fractionation by heating, which is known to negatively impact bio-oil.

Results and Discussion

We have developed a new reaction/separation concept based on a family of recoverable nano-hybrid catalysts that simultaneously stabilize emulsions in biphasic bio-oil. These nanostructured solid particles exhibit a unique advantage in streamlining biomass refining, where the immiscibility and thermal instability of crude bio-oil greatly complicates purification procedures. These novel catalyst/emulsifier hybrids can catalyze reactions with high "phase-selectivity" either in the aqueous or organic phases.

These catalysts are obtained by fusing carbon nanotubes with metal-oxide particles, which results in two-faced nanohybrid solids that are able to stabilize water/oil emulsions by forming a rigid film at liquid-liquid interface of the droplets and increasing the apparent viscosity of the system (1).

The metal oxide in the nanohybrid acts both, as the hydrophylic side of the emulsifier, and as a catalyst for condensation reactions in the aqueous phase. Accordingly, small oxygenates soluble in water, with low fuel value, condense via aldol-condensation, ketonization, or etherification resulting in products, which are no longer water-soluble molecules and therefore migrate to the organic phase. The oxide used can vary in acid/base characteristics. Some of the metal-oxides tested are; MgO, SiO_2, TiO_2 and ZnO.

In the organic phase, transition metals such as Pd, Ni and Cu have been deposited onto the hydrophobic carbon nanotube of the nanohybrids to catalyze deoxygenation reactions including hydrogenation, hydrogenolysis, or decarbonylation occurring on the oil side of the emulsion.

Table 1 shows an example of deoxygenation reactions conducted in the biphasic system stabilized by the nanotube/silica hybrids and loaded with Pd catalyst. The reaction was conducted in a semibatch Parr reactor in the presence of flowing hydrogen gas at 900 psig. As summarized in the table, as the reaction temperature increased, the dominant reaction shifted from hydrogenation to hydrogenolysis and to decarbonylation. Depending on the water/oil partition coefficients, the products were observed in the oil or water phases, respectively. The more deoxygenated products were collected in the oil phase. The example demonstrates the potential of this novel system to conduct simultaneously reaction at the water/oil interface and separation based on the significant differences in water/oil partitions of the deoxygenation products.

Table 1. Variation of product distribution and partition of the products in the water and oil phases as a function of reaction temperature.

Product	Reaction	Yield (%) at Reaction Temperature (°C)			Partition in water/ oil
		100	200	250	
Vanillin	Feed	13.3	0.1	0	80/20
Vanillin Alcohol	Hydrogenation	46.7	0	0	78/22
4-methoxy-2-methyl phenol	Hydrogenolysis	40.0	93.9	8.0	5/95
2-methoxy phenol	Decarbonylation	0	6.0	92.0	15/85

Conclusions

We have accomplished biphasic hydrodeoxygenation and condensation catalysis in high yields, using these nono-hybrid catalysts for several systems of interest in biomass refining (2). Reactions were conducted in a semi-batch reactor with the liquid composed of three layers oil/emulsion/water and with continuous flow of hydrogen, at temperatures in the range 80-250°C, and pressures (300-900 psi) high enough to maintain the water in the liquid state.

References

(1) M. Shen, D. E. Resasco, *Langmuir*, 25, 10843 (2009).
(2) S. Crossley, J. Faria, M. Shen and D. E. Resasco, *Science*, 327, 68 (2009).